Hindawi
Mathematical Problems in Engineering
Volume 2018, Article ID 3980790, 11 pages
https://doi.org/10.1155/2018/3980790

Research Article

The Resonance Reliability and Global Sensitivity Analysis of Curved Pipe Conveying Fluid Based on TIS Method

Zhao Yuzhen,[1] **Liu Yongshou**,[1] **Guo Qing**,[1] **and Li Baohui**[2]

[1]*School of Mechanics, Civil Engineering and Architecture, Northwestern Polytechnical University, Xi'an, Shaanxi 710129, China*
[2]*College of Water Resources and Architectural Engineering, NORTHWEST A&F UNIVERSITY, Yangling, Shaanxi 712100, China*

Correspondence should be addressed to Liu Yongshou; yongshouliu@nwpu.edu.cn

Received 6 August 2018; Accepted 14 November 2018; Published 28 November 2018

Academic Editor: Elena Zaitseva

Based on the Flügge curved beam theory and total inextensible assumption, the dynamic equations of curved pipe's in-plane vibration are established using the Newton method. The wave propagation method is proposed for calculating the natural frequency of curved pipes with clamped-clamped supported at both ends. Then, the performance function of the resonance reliability of curved pipe conveying fluid is established. Main and total effect indices of global sensitivity analysis (GSA) are introduced. The truncated importance sampling (TIS) method is used for calculating these indices. In the example, the natural frequency and critical velocity of a semicircular pipe are calculated. The importance ranking of input variables is obtained at different working conditions. The method proposed in this paper is valuable and leads to reliability estimation and antiresonance design of curved pipe conveying fluid.

1. Introduction

Curved pipes conveying fluid are widely used in aerospace, aircraft, nuclear, petroleum, and ocean engineering. All kinds of uncertainties in fluid velocity, pressure, pipe geometry, and materials will lead to a large change on the natural frequency of the curved pipe conveying fluid through the fluid-structure interaction. When the natural frequency is close to the excitation frequency, this will lead to the resonance failure of pipes. The resonance will have a large damage to the curved pipe. So it is essential and important to study the resonance reliability analysis of curved pipe conveying fluid.

Up to now, there have been a lot of researches in solving the natural frequency of curved pipes conveying fluid [1–10]. Chen S.S. [2] put forward the semicircular pipe's vibration dynamic model. In this model, the total axial extension is none, and the Newton and Hamilton method is used to deduce the motional differential equation of curved pipes conveying fluid. Ni Q. et al. [3] have a lot of work in the dynamic researching of curved pipes. They used the differential quadrature method (DQM) to study the semicircular pipe's vibration and stability analysis. Misra A.K. et al. [4, 5] used the finite element method (FEM) to study the dynamics and stability of curved pipes conveying fluid. Li B.H. et al. [6] put forward the wave propagation method to solve the natural frequency of curved pipes, including the total extensible assumption and total inextensible assumption. Based on the Hamilton principle, Jung D.H. et al. [7] put forward the novel expression of fluid acceleration of semicircular pipe. Hu J.Y. et al. [8] studied the fluid-conveying curved pipe with an arbitrary undeformed configuration.

Although researchers have made a lot of progress in vibration analysis of pipes conveying fluid, the study of resonance failure of pipes conveying fluid is scarce [9–12]. Nokland T.E. et al. [9] provided a guideline for selecting the appropriate importance measure for different application of risk and reliability. Kvassay M. et al. [10] proposed a new approach for importance analysis of multistate Systems (MSSs). Zhai H.B. et al. [13] studied the dynamic reliability of straight pipe conveying fluid based on a refined response surface method, but the pipe is uniformly straight. Alizadeh A.-A. et al. [14] used the Monte Carlo method to study the self-vibration and stability analysis of fluid-conveying pipe. Li Y.L. et al. [15] computed the reliability of subsea under

spatially varying ground motions by using subset simulation. Among these researches, only the single straight pipe was considered for calculating the resonance failure and local sensitivity analysis (LSA). Then random parameters such as pipe length and diameter and fluid density are considered and the reliability of fuel pipelines in different flight states using different gradual enlarged pipes is analyzed. Sensitivity of the fuel pipeline's functional reliability is explored, and pipe length is chief factor with influences on functional reliability. The parameter sensitivity has been also analyzed by Monte Carlo method. They also studied the parameter sensitivity of the metal bellows based on Monte Carlo method. But the fluid-structure interaction was not considered. Ritto T.G. et al. [16] proposed a probabilistic model for the fluid-structure interaction considering modeling errors and analyzed the stability of the stochastic system. Yun W.Y. et al. [17] proposed a modification to the importance sampling in reliability analysis.

The resonance failure is getting more and more serious in engineering especially in the pipe systems. But there are few papers studying the resonance failure of the pipes conveying fluid especially for the curved pipe. Because the curved pipes are widely used in engineering, studying the resonance failure of curved pipes conveying fluid is essential and important. There are many input variables affecting the failure probabilities and the uncertainty of each variable has different effects on the resonance failure probability. The sensitivity analysis aims to measure the uncertainty of each input variable on the failure probabilities including local sensitivities analysis (LSA) and global sensitivity analysis (GSA). Compared to the LSA, the GSA reflects the effect of the variable's distribution on the failure probabilities globally. Many global sensitivity analyses such as the variance-based GSA and moment independent GSA are available. This work is proposed for reducing the failure probability of curved pipes conveying fluid, so the global reliability sensitivity indices defined by Cui L.J. [18] and Li L.Y. [19] can be used in this paper. The main and total effect indices are introduced. The failure probability can be reduced mostly by decreasing the uncertainty of input variables with high main effect indices, and the failure probabilities cannot be reduced significantly by decreasing the uncertainty of the input variables with small total effect induces close to zero [20]. This can help designers reduce the pipe's resonance failure probabilities. This work aims at studying the effect of the uncertainty of each input variable on the resonance failure probability and deciding how to reduce the failure probability by decreasing the uncertainty of the input variables.

This paper is organized as follows: Section 2 introduces the wave propagation method for calculating the natural frequency of curved pipes conveying fluid. Section 3 establishes the performance function of resonance reliability of curved pipes conveying fluid. The resonance reliability and Sobol's variance-based GSA based on the TIS method are introduced. Section 4 calculates the resonance reliability and Sobol's variance-based main and total effect indices of the clamped-clamped supported curved pipe conveying fluid. Section 5 gives the conclusion to this work.

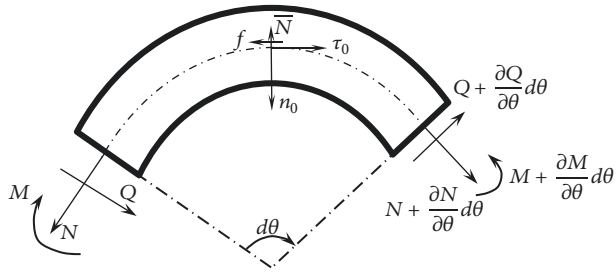

Figure 1: The force sketch of curved pipe.

2. Motion Equations

There are two assumptions of approximating curved pipe, i.e., the total extensible assumption and total inextensible assumption. In this paper, on the base of total inextensible assumption, the Flügge curved beam was applied, and the wave propagation method is proposed for calculating the natural frequency of in-plane vibration.

2.1. Dynamic Equations of In-Plane Vibration. The force diagram of the pipe is sketched in Figure 1. The N, Q, and M are the axial force, shear force, and bending moment along the pipe, respectively. $\overline{N}$ and f denote normal and shear force of the unit fluid acting on the pipe, as shown in Figure 1.

The equilibrium equation along the tangent line is as follows:

$$\left(N + \frac{\partial N}{\partial \theta} d\theta\right) \cos \frac{d\theta}{2} - N \cos \frac{d\theta}{2} + \left(Q + \frac{\partial Q}{\partial \theta} d\theta\right) \sin \frac{d\theta}{2} + Q \sin \frac{d\theta}{2} - fRd\theta = \rho_p A_p Rd\theta \frac{\partial^2 u}{\partial t^2} \quad (1)$$

where $ds = Rd\theta$, $\partial/\partial\theta = R(\partial/\partial s)$, $\cos(d\theta/2) \doteq 1$, and $\sin(d\theta/2) \doteq d\theta/2$. Equation (1) can be simplified as

$$\frac{\partial N}{\partial s} + \frac{Q}{R} - f = m_p \frac{\partial^2 u}{\partial t^2} \quad (2)$$

where $m_p = \rho_p A_p$ is the unit mass of the curved pipe.

The equilibrium equation along the normal line is

$$\frac{N}{R} - \frac{\partial Q}{\partial s} - \overline{N} = m_p \frac{\partial^2 w}{\partial t^2} \quad (3)$$

The moment equilibrium equation is

$$\frac{\partial M}{\partial \theta} d\theta + QRd\theta = 0 \quad (4)$$

Equation (4) also can be written as

$$\frac{\partial M}{\partial s} + Q = 0 \quad (5)$$

The force diagram of fluid is sketched as Figure 2. In this paper, the pressure dropping along the pipe is neglected. P is

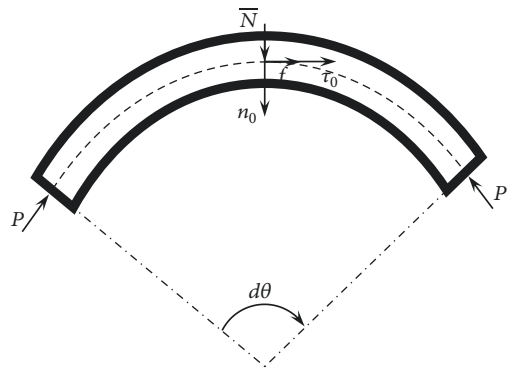

Figure 2: The force sketch of the fluid.

the pressure on the cross section, and $\mathrm{P} = PA_f$. The pressure is along the direction of minus tangent line of the pipe axial, and $\mathrm{P} = -\mathrm{P}\tau$.

The relationship of coordinate systems before and after deformation is

$$\begin{pmatrix} \tau \\ n \end{pmatrix} = \begin{bmatrix} 1 & \frac{u}{R} + \frac{\partial w}{\partial s} \\ -\frac{u}{R} - \frac{\partial w}{\partial s} & 1 \end{bmatrix} \begin{pmatrix} \tau_0 \\ n_0 \end{pmatrix} \tag{6}$$

Combining P and (6), the pressure P can be written as

$$\mathrm{P} = \mathrm{P}\tau_0 + \mathrm{P}\left(\frac{u}{R} + \frac{\partial w}{\partial s}\right) n_0 \tag{7}$$

Then, the equilibrium equation along the tangent line can be written as

$$\begin{aligned} &\mathrm{P}\cos\frac{d\theta}{2} + \mathrm{P}\left(\frac{u}{R} + \frac{\partial w}{\partial s}\right)\sin\frac{d\theta}{2} - \mathrm{P}\cos\frac{d\theta}{2} \\ &+ \mathrm{P}\left(\frac{u}{R} + \frac{\partial w}{\partial s}\right)\sin\frac{d\theta}{2} + fRd\theta = \rho_f A_f Rd\theta a_{\tau_0} \end{aligned} \tag{8}$$

Equation (8) can be simplified as

$$\frac{\mathrm{P}}{R}\left(\frac{u}{R} + \frac{\partial w}{\partial s}\right) + f = m_f a_{\tau_0} \tag{9}$$

where $m_f = \rho_f A_f$ is the fluid mass of unit length.

The normal equilibrium equation is

$$\overline{N} - \frac{\mathrm{P}}{R} = m_f a_{n_0} \tag{10}$$

Combining (3), (4), (9), and (10), the fluid and pipe coupled dynamic equations are obtained as follows:

$$\begin{aligned} \text{Tangent}: \ &\frac{\partial N}{\partial s} + \frac{Q}{R} - m_f a_{\tau_0} + \frac{\mathrm{P}}{R}\left(\frac{u}{R} + \frac{\partial w}{\partial s}\right) \\ &= m_p \frac{\partial^2 u}{\partial t^2} \end{aligned} \tag{11}$$

$$\text{Normal}: \ \frac{N}{R} - \frac{\partial Q}{\partial s} - m_f a_{n_0} - \frac{\mathrm{P}}{R} = m_p \frac{\partial^2 w}{\partial t^2} \tag{12}$$

In this paper, the Flügge beam model is used to approximate the curved pipe. The axial force N and the shear force Q are [21, 22]

$$\begin{aligned} N &= EA_p\left(\frac{\partial u}{\partial s} - \frac{w}{R}\right) + \frac{EI}{R}\left(\frac{\partial^2 w}{\partial s^2} + \frac{w}{R^2}\right) \\ &= \frac{EI}{R}\left(\frac{\partial^2 w}{\partial s^2} + \frac{w}{R^2}\right) \\ Q &= EI\left(\frac{\partial^3 w}{\partial s^3} + \frac{1}{R^2}\frac{\partial w}{\partial s}\right) \end{aligned} \tag{13}$$

Because the axial strain $\varepsilon = 0$, the first item of axial force N is zero. E is Young's modulus, and I is the inertia moment across the section.

The fluid acceleration in the pipe can be described as

$$\begin{aligned} a_f = a_{\tau_0}\tau_0 + a_{n_0}n_0 = &\left[\frac{\partial^2 u}{\partial t^2} + V\left(\frac{\partial^2 u}{\partial t \partial s} - \frac{1}{R}\frac{\partial w}{\partial t}\right)\right. \\ &- \frac{V^2}{R}\left(\frac{u}{R} + \frac{\partial w}{\partial s}\right)\Bigg]\tau_0 + \left[\frac{\partial^2 w}{\partial t^2}\right. \\ &\left. + 2V\left(\frac{1}{R}\frac{\partial u}{\partial t} + \frac{\partial^2 w}{\partial t \partial s}\right) + V^2\left(\frac{1}{R} + \frac{1}{R}\frac{\partial u}{\partial s} + \frac{\partial^2 w}{\partial s^2}\right)\right] \\ &\cdot n_0 \end{aligned} \tag{14}$$

Combining (13), (14), (11), and (12), we can get the tangent and normal dynamic equations as follows:

Tangent dynamic equation:

$$\begin{aligned} &\frac{2EI}{R}\left(\frac{\partial^3 w}{\partial s^3} + \frac{1}{R^2}\frac{\partial w}{\partial s}\right) + \frac{1}{R}\left(\mathrm{P} + m_f V^2\right)\left(\frac{u}{R} + \frac{\partial w}{\partial s}\right) \\ &- m_f V\left(\frac{\partial^2 u}{\partial t \partial s} - \frac{1}{R}\frac{\partial w}{\partial t}\right) = \left(m_f + m_p\right)\frac{\partial^2 u}{\partial t^2} \end{aligned} \tag{15}$$

Normal dynamic equation:

$$\begin{aligned} &EI\left(\frac{\partial^4 w}{\partial s^4} - \frac{w}{R^4}\right) + \frac{\mathrm{P}}{R} + 2m_f V\left(\frac{1}{R}\frac{\partial u}{\partial t} + \frac{\partial^2 w}{\partial t \partial s}\right) \\ &+ m_f V^2\left(\frac{1}{R} + \frac{1}{R}\frac{\partial u}{\partial s} + \frac{\partial^2 w}{\partial s^2}\right) \\ &= -\left(m_f + m_p\right)\frac{\partial^2 w}{\partial t^2} \end{aligned} \tag{16}$$

2.2. Solution of the Dynamic Equation. When the motion is simple harmonic vibration, tangential displacement and radial displacement can be written as [21, 22]

$$\begin{aligned} u(s,t) &= C_u \exp i(ks + \omega t), \\ w(s,t) &= C_w \exp i(ks + \omega t) \end{aligned} \tag{17}$$

where $i = \sqrt{-1}$ is the imaginary number unit, k and ω

are the wave number and frequency, and C_u and C_w are the undetermined coefficient.

Substituting (17) into (15), (16) and neglecting the same factor $\exp i(ks + \omega t)$, we can get the matrix as follows:

$$\begin{bmatrix} -\dfrac{2EIik^3}{R} + \left(\dfrac{2EI}{R^3} + \dfrac{\mathrm{P} + m_f V^2}{R}\right) ik & \dfrac{\mathrm{P} + m_f V^2}{R^2} + \left(m_p + m_f\right)\omega^2 \\ EIk^4 - m_f V^2 k^2 - 2m_f V\omega k & \dfrac{2m_f Vi\omega}{R} \\ -\dfrac{EI}{R^4} + \dfrac{m_f V^2}{R^2} - \left(m_p + m_f\right)\omega^2 & \end{bmatrix} \begin{bmatrix} C_w \\ C_u \end{bmatrix} = 0 \tag{18}$$

To solve the equation above, the determinant on the left side of (18) must be nonzero. And a fourth-order polynomial equation is obtained which is called to be the frequency dispersion equation.

$$\begin{aligned} &k^4 - \frac{2\beta\omega}{R\alpha}k^3 - \frac{m_f V^2}{EI}k^2 \\ &\quad + \left(\frac{2\beta\omega}{\alpha R^3} + \frac{\beta\omega\left(\mathrm{P} + m_f V^2\right)}{\alpha REI} - \frac{2m_f V\omega}{EI}\right)k \\ &\quad - \frac{1}{R^4} + \frac{m_f V^2}{R^2 EI} - \frac{\left(m_f + m_p\right)\omega^2}{EI} = 0 \end{aligned} \tag{19}$$

where $\alpha = (\mathrm{P} + m_f V^2)/R^2 + (m_p + m_f)\omega^2$, $\beta = 2m_f V/R$.

Equation (19) has four roots. Two of them are real numbers and are opposite to each other. The others are conjugate numbers for each other. They represent the wave positive and negative propagating along the pipe, respectively. In this paper, k_1 and k_2 are regarded as the negative propagation waves along the curved pipe. k_3 and k_4 are regarded as the positive propagation waves along the curved pipe.

As shown in Figure 3, the positive propagation wave and negative propagation wave along the semicircular pipe with clamped support are described as W^+, W^-. The subscripts l and r are left and right sides of the curved pipe, respectively.

where T_l and T_r represent the left wave propagation and right wave propagation and R_l and R_r are the reflect matrix of left and right wave, it is easy to know that

$$\begin{aligned} W_r^+ &= T_r W_l^+, \\ W_l^- &= T_l W_r^- \end{aligned} \tag{20}$$

The transformation matrices of left and right wave propagation are

$$\begin{aligned} T_l &= \begin{bmatrix} \exp\left(-ik_1 R\pi\right) & 0 \\ 0 & \exp\left(-ik_2 R\pi\right) \end{bmatrix}, \\ T_r &= \begin{bmatrix} \exp\left(ik_3 R\pi\right) & 0 \\ 0 & \exp\left(ik_4 R\pi\right) \end{bmatrix} \end{aligned} \tag{21}$$

The reflection relation on the left side is

$$W_l^+ = R_l W_l^- \tag{22}$$

Combined with (14), (22) could be expanded as

$$\begin{aligned} C_{u1} + C_{u2} + C_{u3} + C_{u4} &= 0 \\ C_{w1} + C_{w2} + C_{w3} + C_{w4} &= 0 \end{aligned} \tag{23}$$

According to the total inextensible assumption $\partial u/\partial s - w/R = 0$, substituting (23) to (17), we can get

$$C_w = RikC_u \tag{24}$$

Substituting (24) into (23), we can get

$$\begin{aligned} C_{u1} + C_{u2} + C_{u3} + C_{u4} &= 0 \\ k_1 C_{u1} + k_2 C_{u2} + k_3 C_{u3} + k_4 C_{u4} &= 0 \end{aligned} \tag{25}$$

$$\begin{bmatrix} 1 & 1 \\ k_1 & k_2 \end{bmatrix} W_l^- + \begin{bmatrix} 1 & 1 \\ k_3 & k_4 \end{bmatrix} W_l^+ = 0 \tag{26}$$

Substituting (22) into (26), the reflect matrix on the left side of the pipe is

$$R_l = -\begin{bmatrix} 1 & 1 \\ k_3 & k_4 \end{bmatrix}^{-1} \begin{bmatrix} 1 & 1 \\ k_1 & k_2 \end{bmatrix} \tag{27}$$

And the reflect matrix on the right side of the pipe is

$$R_r = -\begin{bmatrix} 1 & 1 \\ k_1 & k_2 \end{bmatrix}^{-1} \begin{bmatrix} 1 & 1 \\ k_3 & k_4 \end{bmatrix} \tag{28}$$

The wave propagation and reflection in the pipe can be expressed as follows [23]:

$$\begin{aligned} W_r^+ &= T_r W_l^+, \\ W_r^- &= R_r W_r^+, \\ W_l^- &= T_l W_r^-, \\ W_l^+ &= R_l W_l^- \end{aligned} \tag{29}$$

The equation above can be written as

$$\left(\mathbf{I} - R_l T_l R_r T_r\right) W_l^+ = 0 \tag{30}$$

where $\mathbf{I}$ is the second-order matrix. This equation which has solutions must satisfy

$$\det\left|\mathbf{I} - R_l T_l R_r T_r\right| = 0 \tag{31}$$

It can be seen that (31) includes ω, so the natural frequency can be solved.

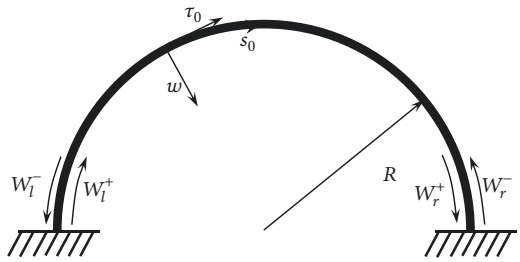

Figure 3: The wave mode in semicircular pipe.

3. Resonance Reliability and GSA

3.1. Performance Function. In order to avoid resonance behavior, the excitation frequency must be far away from the natural frequency of the curved pipe conveying fluid [24, 25]. The resonance failure probability analysis aims to estimate the failure probability of the structure.

In the reality engineering, due to the uncertainties among materials, manufacturing, installing, and servicing, the excited frequency, natural frequency, and vibration response are random variables. According to the traditional design criterion, there exist risks in resonance design if $1 - k_1 < RR/S < 1 + k_2$, where RR is the natural frequency, S is the excited frequency, and k_1 and k_2 are the constants based on the materials. For different materials, k_1 and k_2 are different. Now it is assumed that $S_1 = (1 - k_1)S$, $S_2 = (1 + k_2)S$, where S_1 and S_2 are the minimum and maximum of excitation circular frequency. The performance function of pipe resonance failure [13]:

$$\begin{aligned} z_{jj}(x) &= \left(R_{jj} - S_1\right) \cdot \left(R_{jj} - S_2\right), \quad jj = 1, 2, \cdots, m \\ z(x) &= \left\{z_1(x), z_2(x), \cdots z_m(x)\right\}. \end{aligned} \tag{32}$$

where $z_{jj}(x)$ is the jj-th performance function, x is the basic variables, R_{jj} is the jj-th natural frequency, and m is the number of orders and is also the failure mode number.

The resonance reliability can also be expressed as follows:

$$P_r = P\{z(\mathbf{x}) > 0\} = \int_{z(\mathbf{x})>0} f_{\mathbf{X}}(\mathbf{x}, \boldsymbol{\theta}_{\mathbf{x}})\, d\mathbf{x}. \tag{33}$$

where $f_{\mathbf{X}}$ is the probability density function (PDF) of x and $\boldsymbol{\theta}_{\mathbf{x}}$ are the distribution indices of variable x.

Equation (33) is a nonlinear invisible performance function, so it could not be solved analytically. The equations could be solved by numerical or approximated approach.

3.2. Global Sensitivity Indices. Suppose the limit state function is given as $Y = g(x)$, where $x = (x_1, x_2, \cdots, x_n)$ is the random input variable vector with joint PDF.

The failure domain of this structure system is defined as

$$F = \{x : g(x) < 0\} \tag{34}$$

Suppose the indicator function of this failure domain is given as $I_F(x)$

$$I_F(x) = \begin{cases} 1 & x \in F \\ 0 & x \notin F \end{cases} \tag{35}$$

Then the failure probability can be expressed as

$$P_f = E(I_F) = \int_{R^n} I_F(x)\, f(x)\, dx = \int_F f(x)\, dx \tag{36}$$

A modified version of global reliability sensitivity index defined by Cui in [18] is given as

$$\begin{aligned} \delta_i^P &= E\left(P_f - P_{f|X_i}\right)^2 \\ &= \int_{-\infty}^{+\infty} \left(P_{fY} - P_{f|X_i}\right)^2 f_i(x_i)\, dx_i \end{aligned} \tag{37}$$

where $P_{f|X_i}$ is the failure probability conditional on X_i.

Further, Li proved that

$$\delta_i^P = E\left(P_f - P_{f|X_i}\right)^2 = V(E(I_F \mid X_i)) \tag{38}$$

In GSA, the global sensitivity indices of a group of input variables are defined as main and total effect indices.

The main effect index of the single input variable is defined as

$$S_i = \frac{V(E(I_F \mid X_i))}{V(I_F)} \tag{39}$$

The total effect index of the single input variables is defined as

$$S_{Ti} = 1 - \frac{V(E(I_F \mid X_{\sim i}))}{V(I_F)} = \frac{E(V(I_F \mid X_{\sim i}))}{V(I_F)} \tag{40}$$

where vector $X_{\sim i}$ is the input variables excluding X_i.The Sobol indices satisfied $0 \le S_i \le S_{Ti} \le 1$.

It is easy to know that the larger the main effect index S_i of one input variable, the higher the contribution of input variable X_i on the failure probability P_f. Reducing the uncertainty of X_i, the reduction of failure probability is much more. Obviously, the smaller the total effect index S_{Ti} of one input variable, the lower the contribution of input variables X_i on the failure probability P_f. If the total effect indices of one input variable are small enough or close to zero, the influence of this input variable can be ignored to reduce the dimensionality and save the calculating cost.

Due to the well-known low total expectation,

$$\begin{aligned} S_i &= \frac{V\left(E\left(I_F \mid x_i\right)\right)}{V\left(I_F\right)} \\ &= \frac{E\left(E^2\left(I_F \mid x_i\right)\right) - E^2\left(E\left(I_F \mid x_i\right)\right)}{P_f - P_f^2} \\ &= \frac{E\left(E^2\left(I_F \mid x_i\right)\right) - P_f^2}{P_f - P_f^2} = \frac{D_i - P_f^2}{D} \end{aligned} \tag{41}$$

$$\begin{aligned} S_{Ti} &= 1 - \frac{V\left(E\left(I_F \mid x_{\sim i}\right)\right)}{V\left(I_F\right)} \\ &= 1 - \frac{E\left(E^2\left(I_F \mid x_{\sim i}\right)\right) - E^2\left(E\left(I_F \mid x_{\sim i}\right)\right)}{P_f - P_f^2} \\ &= 1 - \frac{E\left(E^2\left(I_F \mid x_{\sim i}\right)\right) - P_f^2}{P_f - P_f^2} = 1 - \frac{D_{\sim i} - P_f^2}{D} \end{aligned} \tag{42}$$

where $D = V(I_F) = P_f - P_f^2$, $D_i = E(E^2(I_F|x_{\sim i}))$, $D_{\sim i} = E(E^2(I_F|x_{\sim i}))$. Thus for computing S_i and S_{Ti}, we need to calculate D, P_f, P_f^2, D_i, and $D_{\sim i}$.

3.3. TIS for Computing S_i and S_{Ti}. In this paper, the TIS procedure is used to calculate the resonance failure probability. Compared with the other procedure, the TIS procedure can further improve the efficiency of solving.

The basic idea of TIS is as follows: in the standard normal space, the most probable point (MPP) x_{MPP} is computed by the advanced first-order second-moment (AFOSM) procedure; the reliability index is the distance from the MPP to the coordinate origin. Then a hypersphere with radius of β can be obtained, denoted as β-sphere. The indicator function of the outer space of the β-sphere is defined as follows [26]:

$$I_\beta = \begin{cases} 0, & \|x\|^2 < \beta^2 \\ 1, & \|x\|^2 \geq \beta^2 \end{cases} \tag{43}$$

The PDF is truncated by the β-sphere, and the truncated importance sampling density function can be written as

$$h_{tr}(x) = \begin{cases} 0, & \|x\|^2 < \beta^2 \\ \dfrac{1}{P_{h_{tr}}} h_x(x), & \|x\|^2 \geq \beta^2 \end{cases} \tag{44}$$

We can rewrite (33) by introducing importance sampling PDF as follows:

$$\begin{aligned} P_f &= \int \cdots \int_{R^n} I_F(x)\, f_x(x)\, dx \\ &= \int \cdots \int_{R^n} I_F(x) \frac{f_x(x)}{h_x(x)} h_x(x)\, dx \end{aligned} \tag{45}$$

Furthermore, by inducing the indicator function $I_\beta(x)$, the failure probability can be rewritten as

$$\begin{aligned} P_f &= \int \cdots \int_{R^n} I_F(x)\, f_x(x)\, dx \\ &= \int \cdots \int_{R^n} I_F(x)\, I_\beta(x) \frac{f_x(x)}{h_x(x)} h_x(x)\, dx \\ &= E\left[I_F(x)\, I_\beta(x) \frac{f_x(x)}{h_x(x)} \right] \end{aligned} \tag{46}$$

where $\omega_2(x) = I_F(x) I_\beta(x) f(x)/h(x)$ and $P_f = E(\omega_2(x))$. So the term ${P_f}^2$ could be rewritten as

$$\begin{aligned} {P_f}^2 &= \int_{R^{2n}} I_F(x)\, I_\beta(x) \frac{f(x)}{h(x)} h(x)\, I_F\left(x'\right) I_\beta\left(x'\right) \\ &\cdot \frac{f\left(x'\right)}{h\left(x'\right)} h\left(x'\right) dx\, dx' = E\Bigg(I_F(x)\, I_\beta(x) \\ &\cdot \frac{f(x)}{h(x)} I_F\left(x'\right) I_\beta\left(x'\right) \frac{f\left(x'\right)}{h\left(x'\right)} \Bigg) \end{aligned} \tag{47}$$

Generating N samples according to importance sampling PDF, the mean value of samples can be regarded as the expectation value. $\widehat{P}_f$ which is the estimated value of P_f could be computed by

$$\widehat{P}_f = \frac{1}{N} \sum_{k=1}^{N} \frac{I_F\left(x_k\right) I_\beta\left(x_k\right) f_x\left(x_k\right)}{h_x\left(x_k\right)} \tag{48}$$

The TIS method just needs to calculate the samples which are in the outer space of the hypersphere. And the traditional method needs to calculate the limit state function values of all sampling points. So the TIS method is more efficient than the traditional method.

Above all, the following five steps based on TIS can be implemented for computing the S_i and S_{Ti}.

Step 1. Generate $2N$ samples of the input variables by $h(x)$, and distribute them to two $N \times n$ sample matrices A_2 and B_2.

Step 2. Generate another $N \times n$ sample matrix $C_2^{(i)}$. Each column is equal to the corresponding column of B_2 except the i-th column, which is equal to i-th column of A_2.

Step 3. Compute the values of functions $\omega_2(x)$, F_3, and F_4 for each sample in A_2, B_2, and $C_2^{(i)}$; then we can obtain four N-dimensional vectors, i.e.,

$$\begin{aligned} \omega_{2A} &= \omega_2\left(A_2\right), \\ \omega_{2B} &= \omega_2\left(B_2\right), \\ F_{3A} &= F_3\left(A_2, C_2^{(i)}\right), \\ F_{4A} &= F_4\left(B_2, C_2^{(i)}\right) \end{aligned} \tag{49}$$

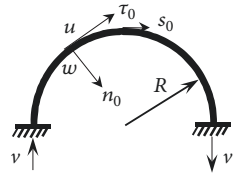

Figure 4: The curved pipe illustration of supported.

Step 4. Compute S_i and S_{Ti} as follows:

$$\widehat{S}_i = \frac{\widehat{D}_i - \widehat{P}_f^2}{\widehat{D}},$$
$$\widehat{S}_{Ti} = 1 - \frac{\widehat{D}_{\sim i} - \widehat{P}_f^2}{\widehat{D}} \tag{50}$$

where $\widehat{P}_f = (1/2N)\sum_{j=1}^{N}(\omega_{2A}^{(j)} + \omega_{2B}^{(j)})$, $\widehat{P}_f^2 = (1/N)\sum_{j=1}^{N}\omega_{2A}^{(j)}\omega_{2B}^{(j)}$, $\widehat{D} = \widehat{P}_f - \widehat{P}_f^2$, and $\widehat{D}_i = (1/N)\sum_{j=1}^{N}F_{3A}^{(j)}$, $\widehat{D}_{\sim i} = (1/N)\sum_{j=1}^{N}F_{4B}^{(j)}$. $\omega_{2A}^{(j)}$, $\omega_{2B}^{(j)}$, $F_{3A}^{(j)}$, and $F_{4B}^{(j)}$ are the j-th element of ω_{2A}, ω_{2B}, F_{3A}, and F_{4B}, respectively. In this step, we first judge if the sample is contained in the β-sphere and if so, then we do not need to compute the limit state function value for this sample.

Step 5. Compute the probable errors of $\widehat{S}_i$ and $\widehat{S}_{Ti}$:

$$\delta\widehat{S}_i \approx \frac{\widehat{D}\delta\widehat{D}_i + \widehat{D}_i\delta\widehat{D}}{\widehat{D}^2},$$
$$\delta\widehat{S}_{Ti} \approx \frac{\widehat{D}\delta\widehat{D}_{\sim i} + \widehat{D}_{\sim i}\delta\widehat{D}}{\widehat{D}^2} \tag{51}$$

where

$$\delta\widehat{D} \approx \frac{0.6745}{\sqrt{N}} \cdot \sqrt{\frac{1}{N}\sum_{j=1}^{N}\left(\frac{\omega_{2A}^{(j)} + \omega_{2B}^{(j)}}{2}\right)^2 - \left(\frac{1}{N}\sum_{j=1}^{N}\left(\frac{\omega_{2A}^{(j)} + \omega_{2B}^{(j)}}{2}\right)\right)^2} \tag{52}$$

$$\delta\widehat{D}_i \approx \frac{0.6745}{\sqrt{N}}\sqrt{\frac{1}{N}\sum_{j=1}^{N}\left(F_{3A}^{(j)}\right)^2 - \left(\frac{1}{N}\sum_{j=1}^{N}\left(F_{3A}^{(j)}\right)\right)^2} \tag{53}$$

$$\delta\widehat{D}_{\sim i} \approx \frac{0.6745}{\sqrt{N}}\sqrt{\frac{1}{N}\sum_{j=1}^{N}\left(F_{4B}^{(j)}\right)^2 - \left(\frac{1}{N}\sum_{j=1}^{N}\left(F_{4B}^{(j)}\right)\right)^2} \tag{54}$$

4. Example

The curved pipe is sketched in Figure 4, and the pipe is clamped-clamped supported at both ends. The materials and geometry are listed in Table 1. Each input variable is independent of others and has the same coefficient of variance.

Table 1: The distribution parameter of the input variables of example.

Input variables/unit	Distribution	Mean value	variance
Pipe Yang's modulus(GPa)	Gauss	68.9	3.43
Pipe outer diameter(m)	Gauss	0.0232	0.00116
Pipe thickness(m)	Gauss	0.0041	0.000205
Pipe density(kg/m3)	Gauss	7197	359.85
Fluid density(kg/m3)	Gauss	1000	50
Velocity(m/s)	Gauss	0	0.05
Maximum excitation frequency(rad/s)	Gauss	410	20.5
Minimum excitation frequency(rad/s)	Gauss	210	10.5
Radius of curvature(m)	Gauss	0.5	0.025
Pressure(MPa)	Gauss	10	0.5

Table 2: The relationship of four natural frequencies and velocities.

V (m/s)	First (rad/s)	Second (rad/s)	Third (rad/s)	Fourth (rad/s)
0	165.46	501.67	992.99	1644.95
10	165.41	501.53	992.83	1644.78
30	165.01	500.42	991.51	1643.36
50	164.22	498.19	988.88	1640.52
100	160.65	487.64	976.43	1627.14

Table 3: The resonance failure probability of curved pipe conveying fluid at different velocity conditions.

Working condition	First failure probability	Second failure probability
v=0 m/s	0.0071463	0.0231528
v=10 m/s	0.0070448	0.0308182
v=20 m/s	0.0062525	0.0373823

4.1. Natural Frequency and Critical Velocity. The first four natural frequencies are listed in Table 2. It is shown from Figure 5 that with increasing of velocity, the natural frequency decreases slowly until the point about $V = 135.1m/s$, where the natural frequency falls to zero suddenly. It means that the critical velocity is $V_{cr} = 135.1m/s$.

4.2. The Resonance Reliability Analysis. The input variables are listed in Table 1, and all the input variables follow the normal distribution. The coefficient of variance ζ is 0.05, the pressure p is 10MPa, the maximum excitation circular frequency $s2$ is 410rad/s, and the minimum excitation circular frequency $s1$ is 210rad/s. Here, different working conditions are considered, $v = 0m/s$, $v = 10m/s$, and $v = 20m/s$. The resonance failure probabilities under different conditions are listed in Table 3.

It can be seen from Table 3 that, with increasing of velocity, the first-order resonance failure probability decreases, and the second-order resonance failure probability becomes

Table 4: The sobol indices with different coefficients of variance.

ζ	index	E	wd	hd	pd	fd	v	$s1$	$s2$	R	p
0.05	$\widehat{S}_i$(E-5)	0.6528	8.4508	6.6361	477.4792	6.1049	0.2442	8414.9	9.0357	475.8557	0.3755
	$\widehat{S}_{Ti}$	0.4032	0.5625	0.2930	0.2784	0.3987	0.4590	0.9991	0.4626	0.8455	0.2553
0.1	$\widehat{S}_i$	0.0796	0.1262	0.00085	0.09031	0.00043	0	0.1038	0	0.0697	0
	$\widehat{S}_{Ti}$	0.09796	0.38659	0.0319	0.20620	0.08094	0.0983	0.80845	0.0890	0.58185	0.09839

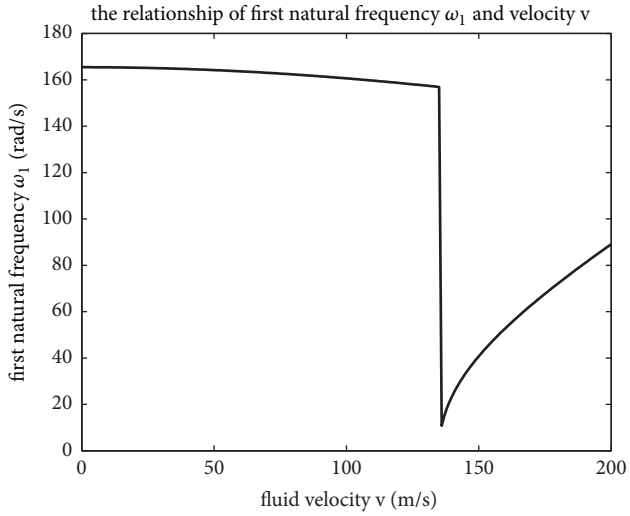

Figure 5: The first natural frequency and velocity relationship.

larger. This is because the natural frequency is decreasing along with the increasing of velocity as shown in Table 2. So the first-order failure area is decreasing, and the second-order failure area is increasing. The results in this example coincide with the theoretical analysis.

4.3. GSA. Table 4 shows the Sobol indices with different coefficients of variance 0.05 and 0.1. Under the working condition, fluid velocity $v = 0m/s$, pressure $p = 10MPa$, the range of excitation circular frequency $s1-s2 : 210-410rad/s$, and the first natural frequency resonance failure probabilities are calculated with the coefficients of variance 0.05 and 0.1. The results are listed in Table 4, where the resonance failure probabilities are $P_{f,\zeta=0.05} = 7.0448\text{E} - 4$ and $P_{f,\zeta=0.1} = 0.1445$, respectively. The results demonstrate that, with the increasing of variance, the failure probability is increasing sharply. The main effect indices are getting larger with the increasing of variance from 0.05 to 0.1. The total effect indices are getting smaller with the increasing of variance. This is because the failure area is getting larger with the increasing of variance, and the resonance failure probability is getting bigger. According to the definition of total effect indices, the total effect indices are inversely proportional to the main effect indices, as demonstrated in Figure 6.

From Figure 6, it can be seen that importance ranking of the main effect indices is $S1 > pd > R > S2 > wd > hd > fd > E > p > v$. It indicates that, by decreasing the uncertainty of $s1$, the failure probability can be reduced most, which is followed by pipe density pd, while the last one is radius of curvature R. The other main effect indices are nearly zero. The failure probability will not change as we reduce the variance of input variable which has small main effect indices close to zero. In the reliability design of curved pipe, we can omit the uncertainty of the input variable which has small main effect indices. In this way we can reduce the dimension of model inputs. The importance ranking based on total effect indices is obtained as follows: $S1 > R > wd > S2 > v > E > fd > hd > pd > p$, and in the total effect indices, none of the indices is close to zero. Obviously, the total indices are larger than main indices, which validates that the interactions along the variables affect the failure probability greatly.

When the coefficient of variance is 0.1, the main effect indices change. Particularly the main index of out pipe diameter wd changes quite a lot. It is demonstrated that the uncertainty of wd will have much more influence on the failure probability. This is because the change of wd will have a lot of influence on the moment of inertia of the cross section. And the changes of moment of inertia will make the mass term change a lot in the motion equations.

Figure 7 shows the Sobol indices with different velocities $v = 0m/s$, $v = 10m/s$, and $v = 30m/s$. From Figure 7, it is shown that the velocity has little effect on the main and total effect indices, because the natural frequency is not obviously relevant to the velocity.

When the velocity increases from 0 m/s to 30 m/s, the main and total effect indices remain unchanged almost. The importance ranking under three velocity conditions still remains as $S1 > pd > R > S2 > wd > hd > fd > E > p > v$. The other main effect indices are close to zero. It indicates that, by decreasing the uncertainty of $s1$, the failure probability can be reduced most, which is followed by pipe density pd, while the last one is radius of curvature R.

From Table 5, the total effect indices stay unchanged with the increasing of velocity. In the total effect indices, none of the indices is close to zero. Obviously, the total indices are larger than main indices, which validates that the interactions along the variables affect the failure probability greatly.

Table 6 shows the main and total effect indices with different two pressures: 0MPa and 10MPa. When the pressure is $p = 0MPa$, the importance ranking of main effect indices is $S1 > R > pd > fd > hd > wd > v > S2 > E > p$. It indicates that, by decreasing the uncertainty of $s1$, the failure probability can be reduced most, which is followed by radius of curvature R, while the last one is pipe density pd. The importance ranking of total effect indices is $S1 > R > v > hd > fd > E > S2 > p > wd > pd$, and none of the input variables is close to zero. Obviously, the total indices are larger than main indices, which validates that the interactions along the variables affect the failure probability greatly.

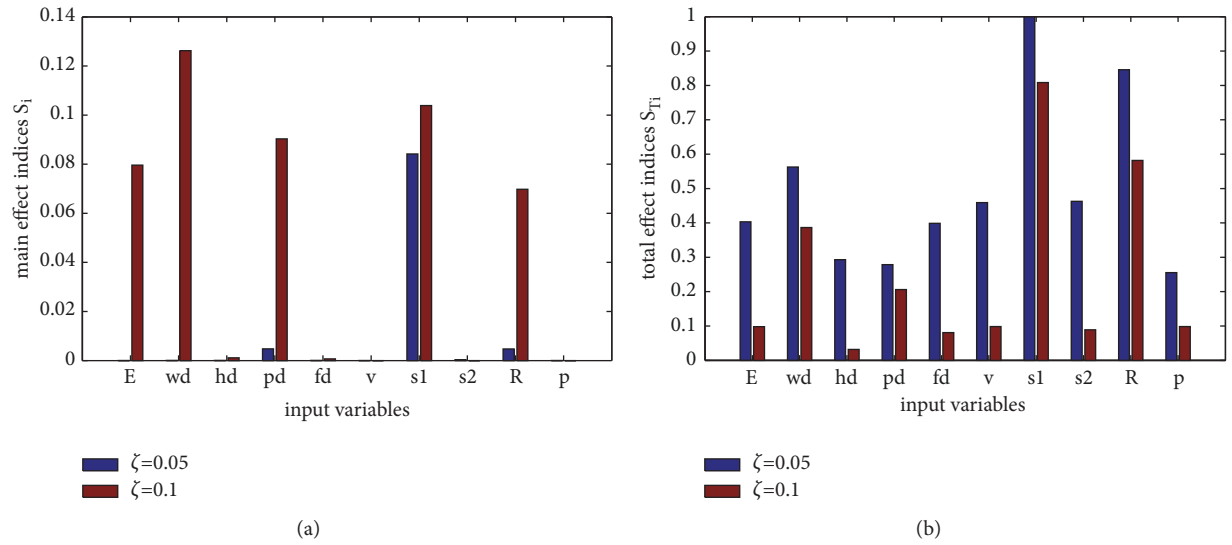

Figure 6: The Sobol indices of different coefficient of variance: main effect indices (a) and total effect indices (b).

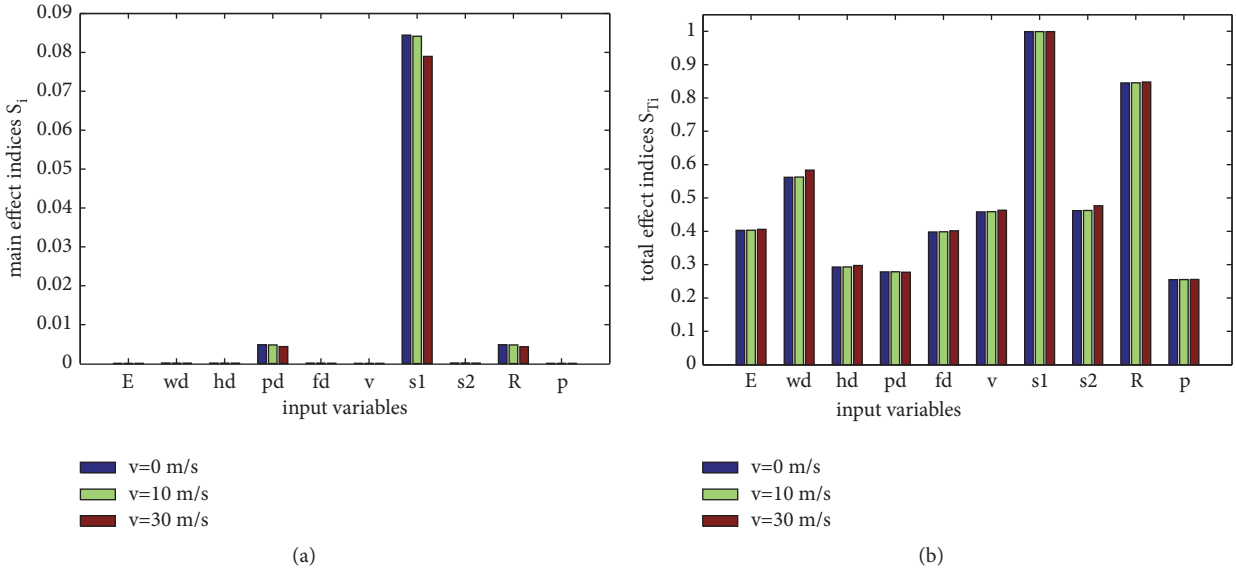

Figure 7: The Sobol indices of different velocity: main effect indices (a) and total effect indices (b).

From Figure 8, it could be concluded that, with the increasing of pressure, the importance ranking will have a big change. Because the pressure has much influence on the pipe's dynamic equation, when the pressure fluctuates, the natural frequency and the resonance failure probability will change a lot.

5. Conclusion

In this paper, the uncertainty of input variables on the natural frequency of the curved pipe conveying fluid is considered. The resonance failure probability and Sobol's GSA are calculated based on TIS method. By decreasing the uncertainty of input variables with high main effect indices, the most reduction of failure probability can be obtained. By decreasing the uncertainty of the input variables with small total effect indices close to zero, the failure probability will not be reduced significantly. Different velocity and pressure working conditions are calculated, respectively.

According to the results of natural frequency, with the increasing of velocity, the natural frequency decreases slowly until the velocity $V = 135.1m/s$, where the natural frequency falls to zero suddenly. So the critical velocity of this example is $V_{cr} = 135.1m/s$. From the main and total effect indices, it can be seen that, reducing the uncertainty of minimum excitation frequency $s1$, the radius of curvature R, the outer diameter wd, and the resonance failure probability can be reduced most. The method proposed in this paper will help the designers to reduce the resonance failure probability by decreasing the uncertainty of the input variables and will

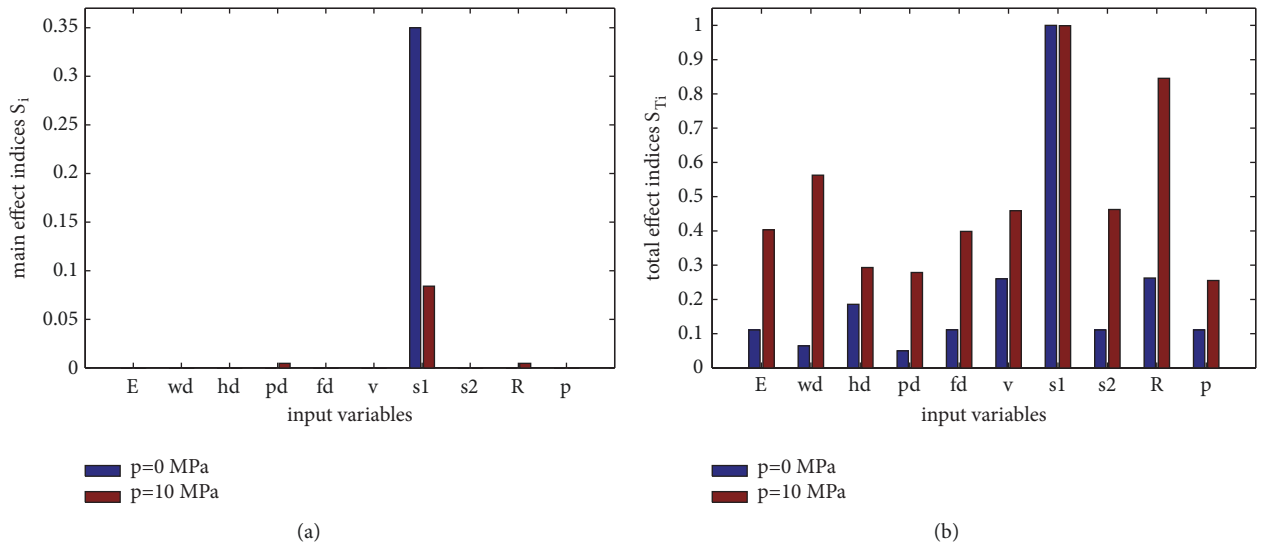

Figure 8: The Sobol indices with different pressure: main effect indices (a) and total effect indices (b).

Table 5: The resonance reliability GSA with different velocities v.

v	index	E	wd	hd	pd	fd	v	$s1$	$s2$	R	p
0m/s	$\widehat{S}_i$	6.651E-6	8.603E-5	6.752 E-5	4.834E-3	6.211 E-5	2.494E-6	8.442E-2	9.195 E-5	4.8215E-3	3.817E-6
	$\widehat{S}_{Ti}$	0.4028	0.5619	0.2926	0.2781	0.3981	0.4582	0.9991	0.4619	0.8452	0.2549
10m/s	$\widehat{S}_i$	6.528e-6	8.450E-5	6.636e-5	4.774E-3	6.105E-5	2.442E-6	8.415E-2	9.035E-5	4.7586E-3	3.755E-6
	$\widehat{S}_{Ti}$	0.40322	0.56258	0.29308	0.27849	0.39877	0.459	0.99913	0.46267	0.8456	0.25537
30m/s	$\widehat{S}_i$	5.6376e-6	7.3446e-5	5.795e-5	0.0043393	5.3316e-5	2.0692e-6	0.078957	7.8782e-5	0.0043244	3.301E-6
	$\widehat{S}_{Ti}$	0.40583	0.58354	0.29737	0.27726	0.4016	0.46314	0.99923	0.47664	0.84785	0.25557

Table 6: The main and total effect indices with different pressures.

p	index	E	wd	hd	pd	fd	v	$s1$	$s2$	R	p
0 Mpa	$\widehat{S}_i$	0	1.935e-85	1.955E-85	2.385E-85	2.35E-85	1.35E-87	0.34995	5.88E-100	4.34E-85	0
	$\widehat{S}_{Ti}$	0.1110	0.06435	0.18587	0.05004	0.111135	0.26033	1	0.11100	0.26248	0.11100
10Mpa	$\widehat{S}_i$	6.528e-6	8.4508e-5	6.6361e-5	0.0047747	6.1049e-5	2.4422e-6	0.08414	9.0357e-5	0.004758	3.7551e-6
	$\widehat{S}_{Ti}$	0.4032	0.5625	0.29307	0.2784	0.3987	0.4590	0.9991	0.4626	0.84559	0.25537

also be guiding for antiresonance designing of curved pipe conveying fluid.

Data Availability

All data included in this study are available upon request by contact with the corresponding author.

Conflicts of Interest

The authors declare that they have no conflicts of interest.

Acknowledgments

The work was supported by the National Natural Science Foundation of China (Grant No. 51505388).

References

[1] M. P. Païdoussis, *Fluid-Structure Interactions: Slender Structures and Axial Flow*, Academic press, London, UK, 2014.

[2] S.-S. Chen, "Vibration and Stability of a Uniformly Curved Tube Conveying Fluid," *The Journal of the Acoustical Society of America*, vol. 51, no. 1B, pp. 223–232, 1972.

[3] Q. Ni, H. L. Zhang, Y. Y. Huang, and Y. P. Chen, "Differential quadrature method for the stability analysis of semi-circular pipe conveying fluid with soring support," *Journal of Engineering Mechanics*, vol. 17, no. 6, pp. 59–64, 2000.

[4] A. K. Misra, M. P. Païdoussis, and K. S. Van, "On the dynamics of curved pipes transporting fluid. Part I: inextensible theory," *Journal of Fluids and Structures*, vol. 2, no. 3, pp. 221–244, 1988.

[5] A. K. Misra, M. P. Païdoussis, and K. S. Van, "On the dynamics of curved pipes transporting fluid. Part II: extensible theory," *Journal of Fluids and Structures*, vol. 2, no. 3, pp. 245–261, 1988.

[6] B. H. Li, H. S. Gao, Y. S. Liu, H. P. Lu, and Z. F. Yue, "Wave propagation method for in-plane vibration of curved pipe

conveying fluid," *Chinese Journal of Solid Mechanics*, vol. 33, no. 3, pp. 302–308, 2012.

[7] D. Jung, J. Chung, and H. H. Yoo, "New fluid velocity expression in an extensible semi-circular pipe conveying fluid," *Journal of Sound and Vibration*, vol. 304, no. 1-2, pp. 382–390, 2007.

[8] Y.-J. Hu and W. Zhu, "Vibration analysis of a fluid-conveying curved pipe with an arbitrary undeformed configuration," *Applied Mathematical Modelling: Simulation and Computation for Engineering and Environmental Systems*, vol. 64, pp. 624–642, 2018.

[9] T. E. Nokland and T. Aven, "On Selection of Importance Measures in Risk and Reliability Analysis," *International Journal of Performability Engineering*, vol. 9, no. 2, pp. 133–147, 2013.

[10] M. Kvassay, E. Zaitseva, and V. Levashenko, "Importance analysis of multi-state systems based on tools of logical differential calculus," *Reliability Engineering & System Safety*, vol. 165, pp. 302–316, 2017.

[11] W. Kuo and X. Zhu, *Importance Measures in Reliability, Risk, and Optimization*, Principles and Applications, Wiley, 2012.

[12] T. Aven, *Risk Analysis: Assessing Uncertainties beyond Expected Values and Probabilities*, Wiley, 2008.

[13] H.-B. Zhai, Z.-Y. Wu, Y.-S. Liu, and Z.-F. Yue, "The dynamic reliability analysis of pipe conveying fluid based on a refined response surface method," *Journal of Vibration and Control*, vol. 21, no. 4, pp. 790–800, 2015.

[14] A.-A. Alizadeh, H. R. Mirdamadi, and A. Pishevar, "Reliability analysis of pipe conveying fluid with stochastic structural and fluid parameters," *Engineering Structures*, vol. 122, pp. 24–32, 2016.

[15] Y. Li, Y. Zhang, and D. Kennedy, "Reliability analysis of subsea pipelines under spatially varying ground motions by using subset simulation," *Reliability Engineering & System Safety*, vol. 172, pp. 74–83, 2018.

[16] T. G. Ritto, C. Soize, F. A. Rochinha, and R. Sampaio, "Dynamic stability of a pipe conveying fluid with an uncertain computational model," *Journal of Fluids and Structures*, vol. 49, pp. 412–426, 2014.

[17] W. Yun, Z. Lu, and X. Jiang, "A modified importance sampling method for structural reliability and its global reliability sensitivity analysis," *Structural and Multidisciplinary Optimization*, vol. 57, no. 4, pp. 1625–1641, 2018.

[18] L. J. Cui, Z. Z. Lü, and X. P. Zhao, "Moment-independent importance measure of basic random variable and its probability density evolution solution," *Science China Technological Sciences*, vol. 53, no. 4, pp. 1138–1145, 2010.

[19] L. Luyi, L. Zhenzhou, F. Jun, and W. Bintuan, "Moment-independent importance measure of basic variable and its state dependent parameter solution," *Structural Safety*, vol. 38, pp. 40–47, 2012.

[20] P. Wei, Z. Lu, W. Hao, J. Feng, and B. Wang, "Efficient sampling methods for global reliability sensitivity analysis," *Computer Physics Communications*, vol. 183, no. 8, pp. 1728–1743, 2012.

[21] S.-K. Lee, B. R. Mace, and M. J. Brennan, "Wave propagation, reflection and transmission in curved beams," *Journal of Sound and Vibration*, vol. 306, no. 3-5, pp. 636–656, 2007.

[22] S. J. Walsh and R. G. White, "Vibrational power transmission in curved beams," *Journal of Sound and Vibration*, vol. 233, no. 3, pp. 455–488, 2000.

[23] C. A. Tan and B. Kang, "Free vibration of axially loaded, rotating Timoshenko shaft systems by the wave-train closure principle," *International Journal of Solids and Structures*, vol. 36, no. 26, pp. 4031–4049, 1999.

[24] S. Q. He and S. Wang, *Structure Reliability Analysis and Design*, Beijing National Defense Industrial Press, 1993.

[25] C. Kuifu and Z. Senwe, "DFT accelaration and its application in non-stationary random vibration calculation," *Journal of Vibration Engineering*, vol. 12, pp. 91–96, 1999 (Chinese).

[26] Z. Z. Lu, S. F. Song, and H. S. Li, *Structure Reliability Analysis and Sensitivity Analysis*, Scientific press, 2009.